

Nonlinear optical correction of the pulse shape from a directly modulated DFB laser

R. Rojas-Laguna ^{a,*}, J. Gutierrez-Gutierrez ^b, E.A. Kuzin ^b, M.A. Bello-Jimenez ^b,
B. Ibarra-Escamilla ^b, J.M. Estudillo-Ayala ^a, A. Flores-Rosas ^b

^a *Universidad de Guanajuato, Facultad de Ingeniería Mecánica, Eléctrica y Electrónica, Apartado Postal 215-A, Salamanca, Gto., C.P. 36730, Mexico*

^b *Instituto Nacional de Astrofísica, Óptica y Electrónica, Luis Enrique Erro No. 1, Departamento de Óptica, Puebla Pue., C.P. 72000, Mexico*

Received 1 July 2007; received in revised form 21 September 2007; accepted 8 October 2007

Abstract

In this work, the effect of modulation instability (MI) in optical fiber is used to reshape nanosecond pulses from a directly modulated diode laser. Our configuration includes a fiber where MI causes the side lobes in the signal spectrum and a filter at the fiber output rejecting the side lobes. Simulations show abrupt drop of the transmission of the setup if pulse power is above some critical value. We investigated the transmission for fibers with lengths in the range between 62-m and 4.5-km. The critical power was found to be inversely proportional to the fiber length. An average scaled critical power is 2.16 W km. We demonstrated the application of the method for rejection of the transient peak in a directly modulated diode laser.

© 2007 Elsevier B.V. All rights reserved.

PACS: 42.65.–k; 42.60.Rn; 42.81.–i

Keywords: Nonlinear optics; Fiber optics; Optical pulse regeneration

1. Introduction

Distributed feedback (DFB) semiconductor lasers have many applications because of their single-mode with high coherence continuous-wave output. These lasers are low cost, small-size, low driving voltage and current [1]. The directly modulated DFB lasers provide very simple method of pulse generation with tuned pulse duration. The performance of the directly modulated laser is limited by the relaxation oscillations in the laser output. Moreover, some amount of current oscillations causes output power oscillation. External modulators are commonly employed because they have much less chirping and relaxation oscillations are eliminated in the output pulse [2]. However, systems using directly modulation are simpler and fairly inexpensive than conventional systems with external mod-

ulation. The directly modulated DFB lasers can be preferable for many applications, such as a master oscillator in high power pulse system made in a master oscillator power amplifier (MOPA) configuration, nonlinear optics, lidars, and sensors (where the laser diode is used as a master oscillator with subsequent amplification) [3–6]. Furthermore, directly modulated DFB lasers with a constant current bias substantially lower than the threshold have a very low level of cw radiation. It allows very high pulse amplification using simple amplifier configurations [4]. However, in the last case relaxation and current oscillations represent a very important issue to be considered.

Recently, some experiments have been carried out to find mechanisms for suppressing the relaxation oscillations of DFB lasers. It was proposed to use external electrical resonant circuits, an optical feedback, light injection (employing GaAs injection lasers), and spontaneous emission [7–10]. Several exhaustive theoretical works analyzing the laser rate equations with the goal to reduce relaxation

* Corresponding author. Tel./fax: +52 464 647 9940x2423.

E-mail address: rlaguna@salamanca.ugto.mx (R. Rojas-Laguna).

oscillations can be found in the literature [11–13]. Some methods using nonlinear all optical reshaping and limiting of signals have been reported recently [14–19]. Most of these methods use optical fibers to take advantage of many nonlinear phenomena that can be observed at moderate powers levels [15]. Four-wave mixing (FWM), self-phase modulation (SPM) and nonlinear couplers are considered for nonlinear optical reshaping [16–19]. All optical reshaping and limiting are considered essentially in the context of the 2R and 3R regeneration of ultrafast optical signals for communication and computing.

In the present work, we propose to use MI for nanosecond pulse reshaping. For the best of our knowledge, it was not discussed before. Modulation instability causes an exponential growth of small perturbations in the power, which consequently produces the side lobes in the spectrum at the fiber output. An essential fraction of the pulse energy is moved to the side lobes and can be rejected by the band pass spectral filter. That causes the limiting effect. We investigate the application of this mechanism for pulse reshaping of nanosecond pulses.

2. Experimental setup

Fig. 1 shows the experimental setup. The 1549 nm input pulse was obtained from the Mitsubishi 925B11F DFB diode laser. The laser was fed from the pulse generator SRS-DG535 that can provide pulses with temporal duration in the range from 1 ns up to several hours. The current pulses were placed on a 6.3 mA bias. The threshold current of the DFB laser was approximately 10.5 mA. The maximum power at the DFB laser output was 5 mW. The coupling efficiency to the fiber was 30%. Pulses from the DFB laser were amplified by a two-stage Erbium-doped fiber amplifier (EDFA) similar to that used in Ref. [4]. The highest gain of the amplifier is 50 dB allowing the 100 W peak power pulses at the EDFA output. A 99/1 coupler was used to monitor pulses entering the fiber under investigation. The EDFA included optical isolators both at the input and at the output. The output pulses were launched to

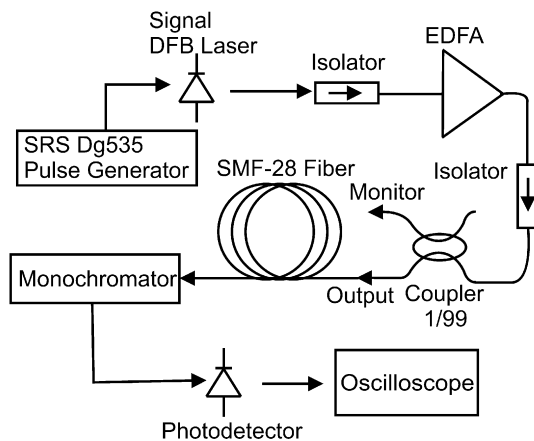


Fig. 1. Experimental setup.

the SMF-28 fiber with dispersion $D = 20$ ps/nm km and nonlinearity $\gamma = 1.52 \times 10^{-3}$ (m W) $^{-1}$. Pulses after the fiber were launched to a monochromator with the resolution of 0.5 nm, detected by a 1-GHz InGaAs photodetector and monitored by a 500-MHz oscilloscope.

Fig. 2a shows the typical pulse shape at the EDFA output. The 30 ns current pulse from the pulse generator was applied that is equal to the optical pulse duration measured as full-width at half-maximum (FWHM). The pulse shows the transient peak and the plateau. The transient peak duration measured as it is shown in Fig. 2a is 2.25 ns. The power of the transient peak is significantly higher than power of the plateau. The ratio between the transient peak power and the plateau power depends on the current from the pulse generator. In our experiments the ratio between the transient peak and the plateau powers was kept approximately as 2:1. The power launched to the investigated fiber was controlled by the EDFA gain. Fig. 2b shows the transient peak measured with a 20-GHz sampling oscilloscope and a 10-GHz detector. Fast relaxation oscillations can be seen.

3. Numerical results

We solved the Eq. (1) for nonlinear pulse propagation in the fiber using the split-step Fourier method [15]. The equation includes the group-velocity dispersion (GVD) term, Kerr nonlinearity, and Raman term.

$$\frac{\partial A}{\partial z} + i \frac{\beta_2}{2} \frac{\partial^2 A}{\partial T^2} = i\gamma |A|^2 A - T_R A \frac{\partial |A|^2}{\partial T}. \quad (1)$$

We used the dispersion with module $|\beta_2| = 25.5$ ps 2 /km and nonlinearity $\gamma = 1.52 \times 10^{-3}$ (m W) $^{-1}$. The used parameters correspond to those for the SMF-28 fiber (GVD is 20 ps/nm km; effective area is 80 μm^2 , $n_2 = 3.2 \times 10^{-20}$ m 2 /W). The variable T represents the physical time in the retarded frame and z is the physical distance. The response time for the Raman term is $T_R = 3$ fs. To model the squared pulse similar to that emitted by the directly modulated diode laser we used for calculations super Gaussian pulses with the waveform given by

$$A(0, T) = \sqrt{P_0} \exp(-(T/T_0)^6), \quad (2)$$

where P_0 is the peak power of the input pulse and T_0 determines pulse duration. The pulse was placed on the noise with normal distribution. The split-step algorithm was used with following parameters: the length of the step was equal to 0.5-m, number of points 2^{14} , and the time window was $-5T_0$ to $+5T_0$.

We calculated the spectrum of MI to determine the wavelength shift of the side lobes maxima and also to determine the wavelength shift at which the side lobe spectrum reaches the value of 0.1 of its maximum. The results are shown in Fig. 3.

The wavelength shift for the maximum is fitted by the square root dependence $\Delta\lambda = 0.46\sqrt{P_0}$. Analytically calcu-

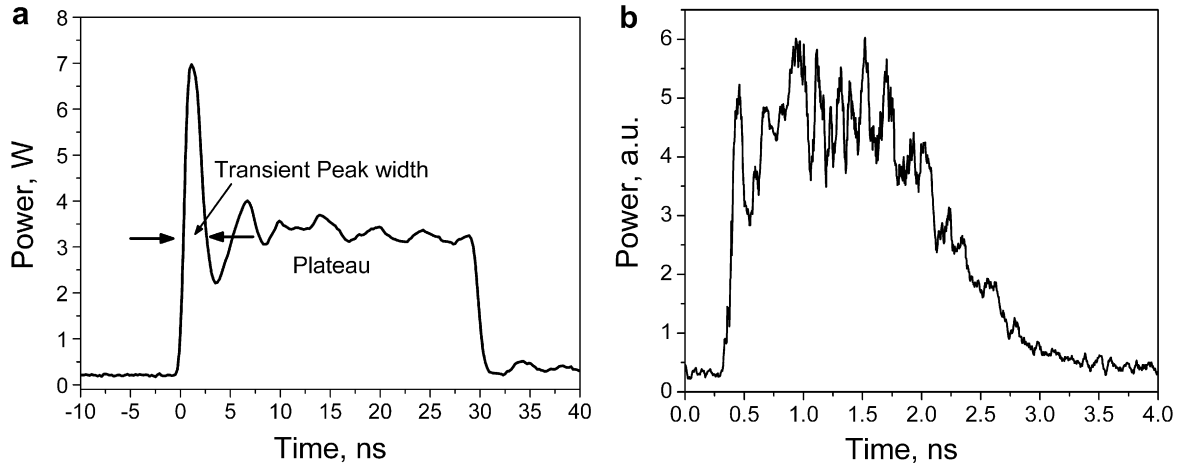


Fig. 2. A typical pulse shape at the EDFA output (a); the transient peak measured with the 10-GHz detector and the 20-GHz oscilloscope (b).

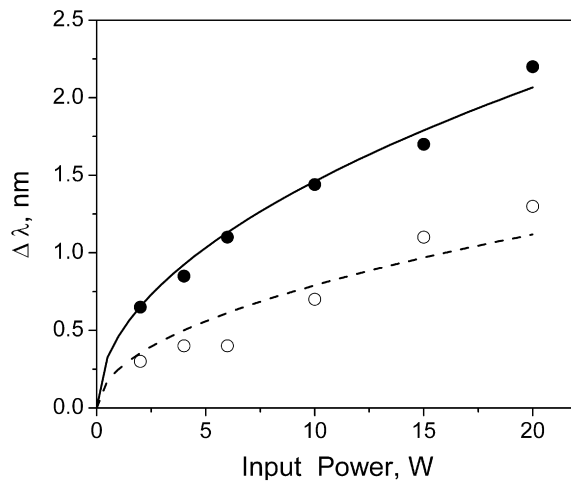


Fig. 3. The wavelength shift of the side lobe maximum, solid circles, and of the 0.1-level of maxima, open circles. The lines give the square root fit $\Delta\lambda = 0.46\sqrt{P_0}$ for maxima and $\Delta\lambda = 0.25\sqrt{P_0}$ for the 0.1-level.

lated maximum of the MI gain [15] gives the value $\Delta\lambda = 0.44\sqrt{P_0}$. Some deviation of the calculated points from the line is caused by stochastic nature of the side lobes that are developed from the noise. Fig. 3 shows, as well, the wavelength shift at which the spectrum of the side lobes reaches the level of 0.1 of its maximum. The calculated points are fitted well by the dependence $\Delta\lambda = 0.25\sqrt{P_0}$. This dependence gives an idea about the filter bandwidth required to reject the side lobes. We used for simulation the filter with FWHM equal to 0.5 nm allowing the rejection of great part of the side lobe power if the input pulse is higher than 1 W.

Fig. 4 shows the energy transmissions for 500-m fiber and pulses with $T_0 = 100$ ps, $T_0 = 300$ ps and $T_0 = 1$ ns. The full pulse duration at the level e^{-1} is respectively 200 ps, 600 ps and 2 ns. The applied noise had the spectral density equal to $1 \mu\text{W}/\text{nm}$ for these dependencies.

For the 600 ps and 2 ns pulses the dependencies have a long plateau with transmission equal to one followed by

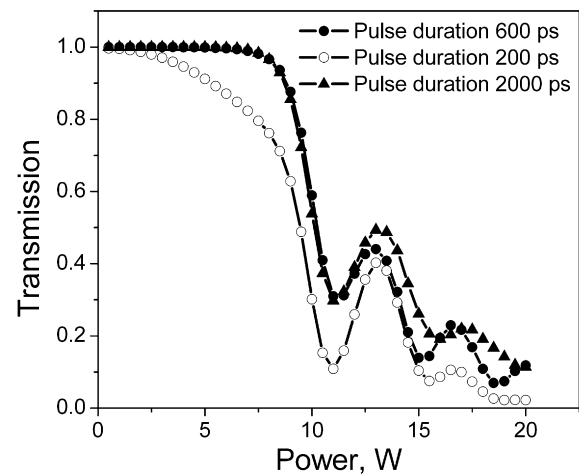


Fig. 4. The calculated transmission for the 500-m fiber.

the dropping part. The transmission reaches the level of 0.9 at 8.8 W, and the level of 0.5 at 10.2 W of the input power. The first minimum of the transmission is reached at 11.5 W. After the first minimum, some oscillation behavior is observed. For short pulses the self-modulation effect begins to play an important role and dependence of the transmission on the input power is changed, see the curve for 200 ps pulses (Fig. 4, open circle). However, Fig. 4 shows that the dependencies for the 600 ps pulse and the 2 ns pulse coincide in the part that is essential for our purposes and we may conclude that for pulses longer than 0.6 ns the transmission does not depend on the duration.

We have found that the Raman term did not cause a significant effect on the transmission. That is due to the decrease of the transmission begins before the pulse is break-up into a set of solitons and the effect of soliton self-frequency shift becomes to be important. However the Raman term makes the long wavelength side lobe slightly higher than the short wavelength side lobe. The time displacement between spectral components for fiber lengths of 4.5-km and shorter and GVD of 20 ps/nm km

is several of tens picosecond. That is essentially less than the peak duration or characteristic time of the oscillations of the power in the plateau. For this reason we may consider that the parts of the pulse act independently. That is true until the strong Stokes component due to SRS appears.

4. Experimental results

We measured the waveforms at the output of the monochromator tuned to the pump wavelength ($\lambda_0 = 1549$ nm). Then, we depicted the dependencies of the output power on the input separately for the peak and for the plateau. Fig. 5 shows the output power against the input power for fiber lengths of 62-m, 210-m and 600-m.

To be able to measure the pulse shape at the monochromator output we used the fast detector with diameter of 100- μ m. Aberrations of the optical system make difficult to collect all light into the active detector area. Instead of doing this, we measured the output power in arbitrary units, however, it is reasonable to consider that for powers sufficiently low the transmission has to be equal to one provided that the bandwidth of the input pulse is less than the bandwidth of the monochromator. The last is true for pulses generated by DFB laser. Therefore we used first

10–15 points of the dependencies to fit the transmission for these points equal to one and then used the same scaling for all point in the curve. Each dependency in Fig. 5 was fit individually. Fig. 6 shows the transmission resulting from this procedure.

To characterize quantitatively the transmission we used the power at which the transmission drops by two times, referred here as the critical power or $P_{0.5}$, and slope of the transmission at the critical power. We found that $P_{0.5}$ is nearly inversely proportional to the fiber length. Fig. 7 shows the values of $P_{0.5}$ times fiber length where the power is measured in Watts and the fiber length is measured in km. We can see that, in the range of the fiber length between 62-m and 4.5-km, the experimental results lies within the range between 1.5 and 2.8 with average value equal to 2.2 W km with the deviation less than 30%. Numerical values depend slightly on the average noise. For the result shown in Fig. 7 we used the average noise equal to 5 mW/nm. In the experiments, the power of the amplified spontaneous emission (ASE) at the EDFA output was in the range between 1 mW and 10 mW depending on the amplification. The ASE spectrum with the bandwidth about 1 nm was centered on the signal wavelength. Fig. 7 shows the reasonable agreement between the simulated and experimental critical powers.

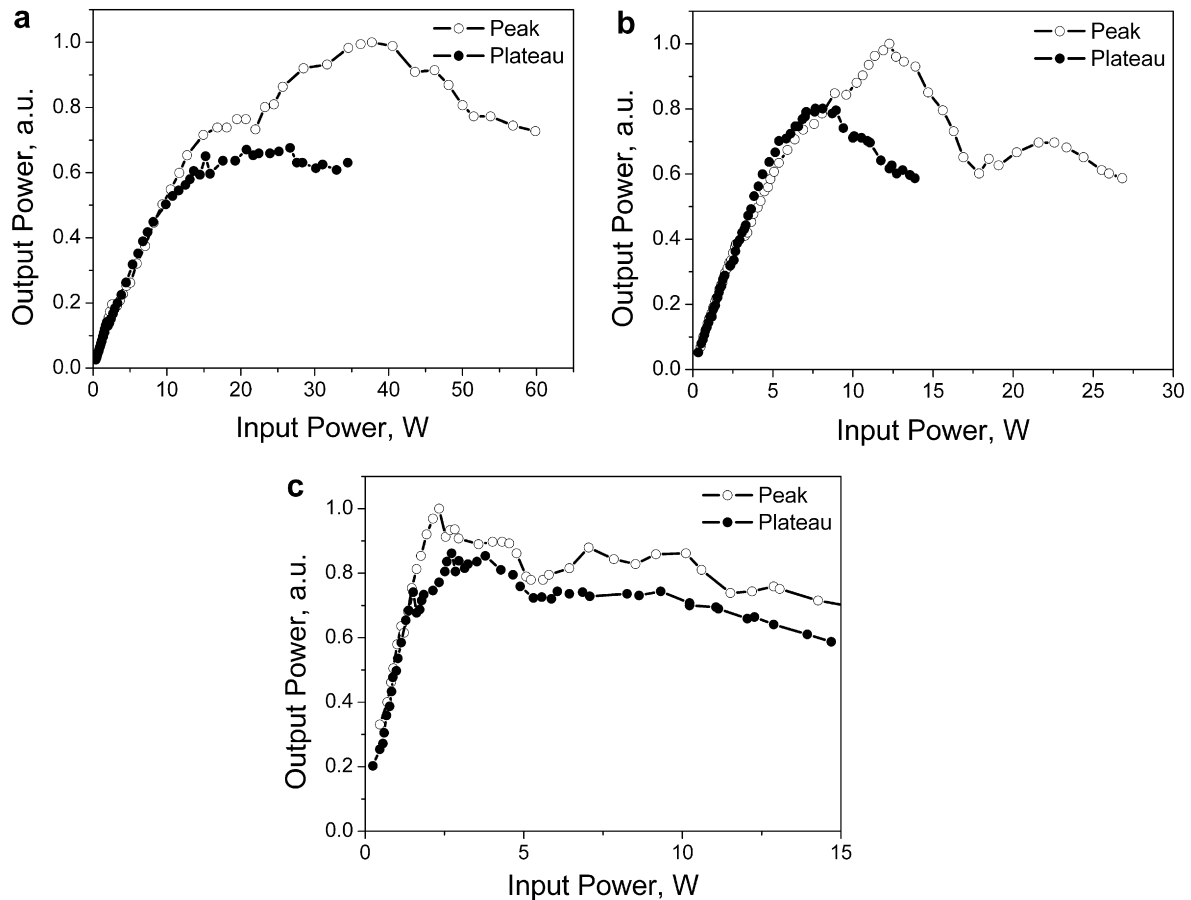


Fig. 5. The output power for 62-m fiber (a), 210-m fiber (b), and 600-m fiber (c).

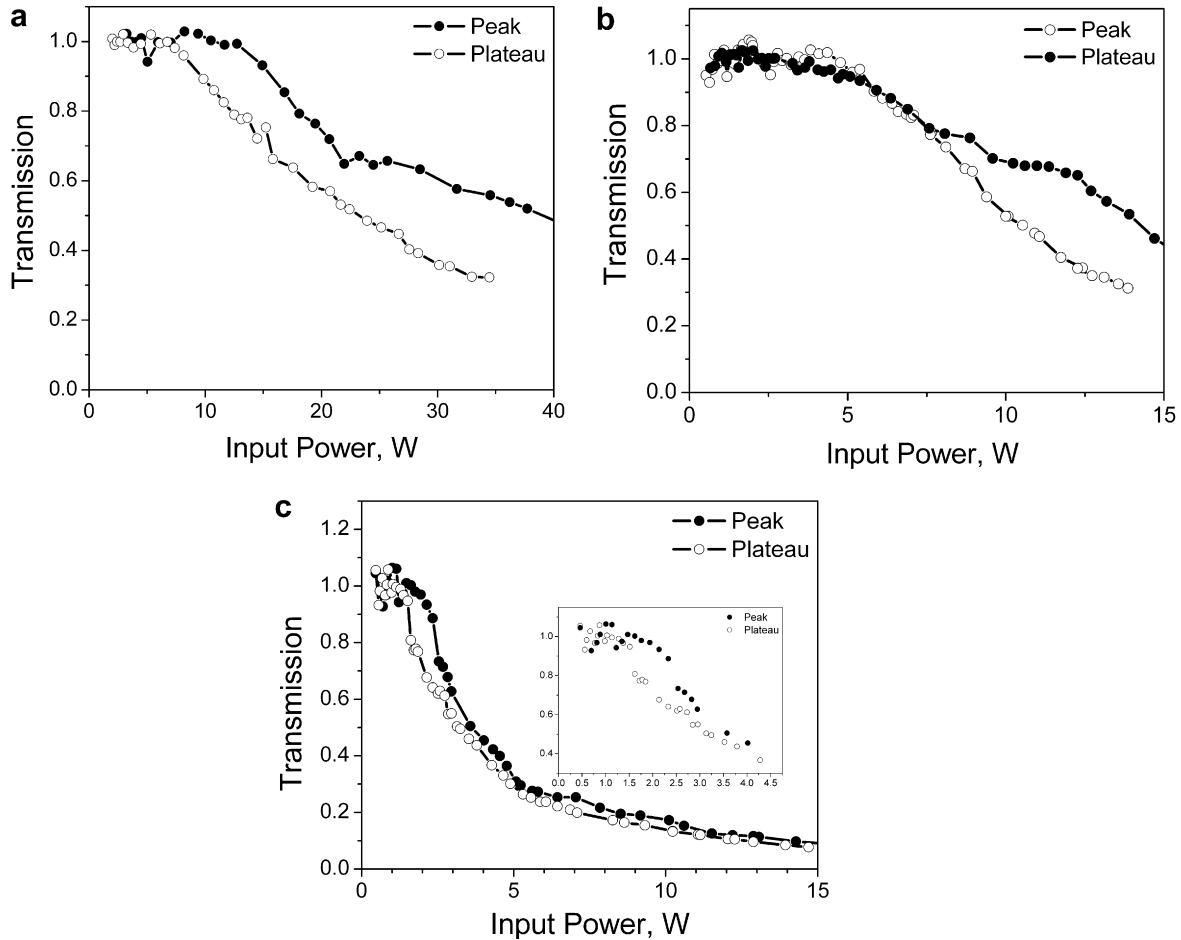


Fig. 6. The transmission for 62-m fiber (a), 210-m fiber (b), and 600-m fiber (c), the inset shows a detail of the curve at low power.

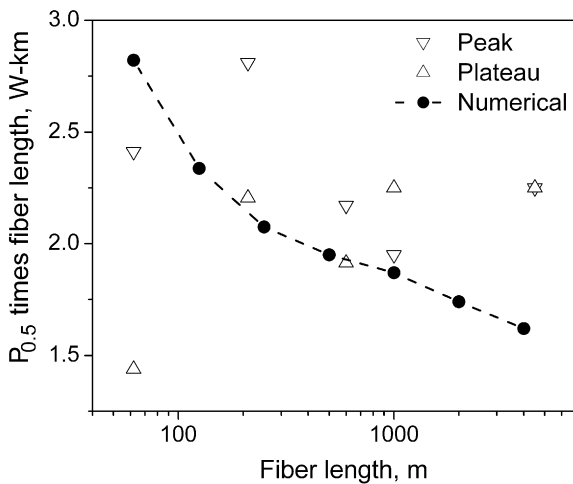


Fig. 7. The $P_{0.5}$ times fiber length.

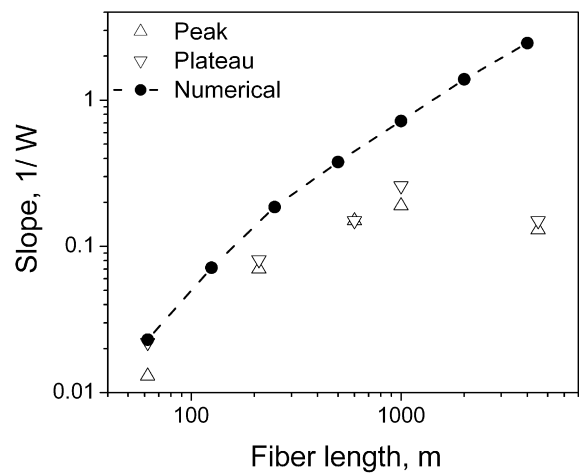


Fig. 8. Slope of the transmission at power equal to $P_{0.5}$.

Fig. 8 shows the experimentally measured and numerically calculated slope of the transmission at the power equal to $P_{0.5}$. The numerically calculated slope is somewhat higher than the measured. The difference grows for longer fiber lengths and reaches an order of value for the 4.5-km fiber. For fibers shorter than 1-km the concordance

between numerical and experimental results can be considered as reasonably good.

To identify the nonlinear process in the fiber we have measured the spectra at the fiber output. Fig. 9 shows some examples of the spectra at the output of the 210-m fiber for the peak and the plateau. Generally the measured spectra

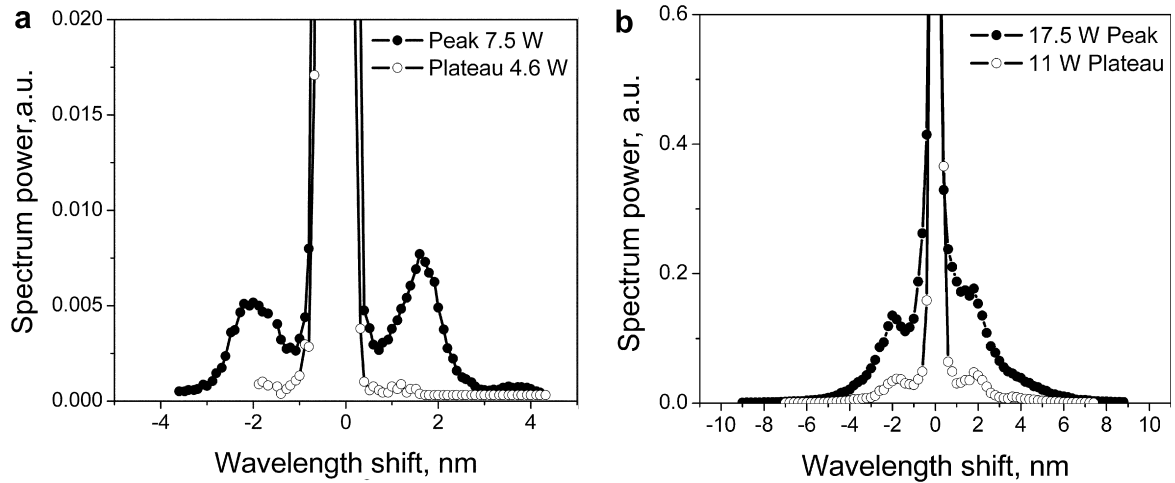


Fig. 9. MI side lobes at different powers for the 210-m fiber.

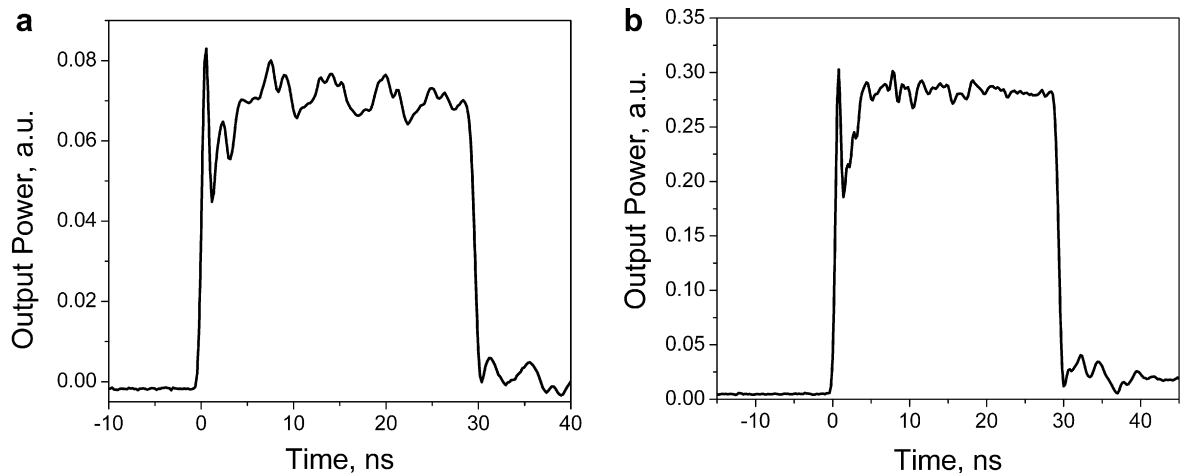


Fig. 10. The pulse shapes at the output of the monochromator.

were similar for the peak and the plateau. The critical power for this fiber was measured to be 10.5 W for the plateau, and 13.4 W for the peak. For input power of 4.6 W that is lower than $P_{0.5}$, the MI side lobes are not detected, see plateau spectrum in Fig. 9a. For the power level close to the critical power the side lobes are very well defined, the 7.5 W peak spectrum in Fig. 9a, and the 11 W plateau spectrum in Fig. 9b. For higher power the side lobes become to be asymmetrical probably because of the Raman effect, see the 17.5 W peak spectrum in Fig. 9b. Each spectrum was scaled to have the maximum value equal to 1.

As an example of the application of the technique we removed the transient peak from the pulse generated by the directly modulated DFB laser. Fig. 10 presents the pulse shapes at the monochromator output after passing the 600-m fiber. For Fig. 10a the powers at the input were 3.5 W and 7 W for the plateau and the transient peak, respectively. We can see that the transient peak is essentially reduced. Fig. 10b shows the pulse shape when the

input powers were 6 W and 12 W for the plateau and the transient peak. The increase of the input power results in more flat pulses at the output, however the power penalty grows for this case.

5. Conclusions

We have demonstrated that generation of spectral side lobes by MI and subsequent filtering can be utilized to correct the waveform of the nanosecond pulses. Experimentally measured dependencies of the transmission show reasonably good correspondence with the numerical calculations using nonlinear equation of propagation including GVD and Kerr nonlinearity. The method requires respectively low powers, several Watts or even less. We demonstrated the application of the method by elimination of the transient peak in the pulses generated by the directly modulated DFB laser.

Acknowledgement

This work was supported by CONACyT Project 47169 and by the Universidad de Guanajuato, Project UGTO-E20325.

References

- [1] Govind P. Agrawal, Niloy K. Dutta, *Semiconductor Lasers*, 2nd ed., International Thompson Publishing, 1993.
- [2] Fumio Koyama, Kenichi Iga, *J. Lightwave Technol.* 6 (1988) 87.
- [3] M. Savage-Leuchs, E. Eisenberg, A. Liu, J. Henrie, M. Bowers, *Proc. SPIE* 6102 (2006) 6102.
- [4] E.A. Kuzin, S. Mendoza-Vazquez, J. Gutierrez-Gutierrez, B. Ibarra-Escamilla, J.W. Haus, R. Rojas-Laguna, *Opt. Express* 13 (2005) 3388.
- [5] C. Allen, Y. Cobanoglu, S. Chong, S. Gogineni, *Proc. IEEE* 4 (2000) 1784.
- [6] G. Whitenett, G. Stewart, K. Atherton, B. Culshaw, W. Johnstone, *J. Opt. A: Pure Appl. Opt.* 5 (2003) 140.
- [7] Y. Suematsu, T.H. Hong, *IEEE J. Quantum Electron.* 13 (1977) 756.
- [8] J.S. Lawrence, D.M. Kane, *IEEE J. Quantum Electron.* 13 (2002) 185.
- [9] C.R. Mirasso, E. Hernandez-Garcia, J. Dellunde, M.C. Torrent, J.M. Sancho, *Opt. Commun.* 115 (1995) 523.
- [10] R. Lang, K. Kobayashi, *IEEE J. Quantum Electron.* 12 (1976) 194.
- [11] J. Chen, R.J. Ram, R. Helkey, *IEEE J. Quantum Electron.* 35 (1999) 1231.
- [12] C. Mayol, R. Toral, C.R. Mirasso, S.I. Turovets, L. Pesquera, *IEEE J. Quantum Electron.* 38 (2002) 260.
- [13] L. Illing, M.B. Kennel, *IEEE J. Quantum Electron.* 40 (2004) 445.
- [14] Z. Xianwei, W. Jianping, *Microwave Opt. Technol. Lett.* 48 (2007) 1606.
- [15] G.P. Agrawal, *Nonlinear Fiber Optics*, Third ed., Academic Press, San Diego, California, 2004.
- [16] M. Matsumoto, *Opt. Express* 14 (2006) 1430.
- [17] E. Ciaramella, S. Trilo, *IEEE Photon. Technol. Lett.* 12 (2000) 849.
- [18] M. Matsumoto, *Optics Express* 14 (2006) 11018.
- [19] Y. Wang, *J. Lightwave Technol.* 17 (1999) 292.